博士論文（要約）

Optimal Attitude and Orbit Control of a Spinning Solar Sail by Spin Rate Control

（スピンレート制御によるスピン型ソーラーセイルの最適姿勢・軌道制御）

大野　剛

Department of Aeronautics and Astronautics

The University of Tokyo

This dissertation is submitted for
the degree of Doctor of Philosophy

2014

Dedication

This thesis is dedicated to my parents, Toru Ono and Miki Ono, for their love, endless support and encouragement.

Acknowledgements

I would like to express the deepest appreciation to my supervisor Dr. Jun'ichiro Kawaguchi for encouraging my research and allowing me to participate in several projects in Japan Aerospace Exploration Agency. Without his supervision and help, this thesis would not have been possible.

I would like to thank my committee members, Dr. Koichi Hori, Dr. Akira Iwasaki, Dr. Ryu Funase and Dr. Makoto Yoshikawa for their kind support and comments on my work. Their suggestions helped me to improve my thesis.

I also would like thank Dr. Osamu Mori, Dr. Yuichi Tsuda, Dr. Takanao Saiki, Dr. Yoji Shirasawa and Dr. Yuya Mimasu. Their advices on my research as well as on my career have been priceless.

I am deeply grateful to Ms. Kazuko Okabe and Ms. Mami Oishi for their support that has enabled me to concentrate on my research.

Special thanks to the students in the laboratory for their company in everyday life. It has been very enjoyable three years thanks to you all.

Finally, I would particularly like to thank my parents, Toru Ono and Miki Ono, for their support and encouragement. They have always been perfect parents for me.

Abstract

Solar sails are a form of spacecraft which deploys a large sail in space and uses solar radiation pressure for propulsion. Solar sailing is considered as an ultimate propulsion system since it does not require any propellant. In 2010, IKAROS developed and launched by Japan Aerospace Exploration Agency (JAXA) has become the first solar sail spacecraft in the world. IKAROS successfully achieved its objective to demonstrate various novel technologies regarding solar sailing: the deployment of a 200 m^2 sail, power generation with thin-film solar cells on the sail, measurement of acceleration due to solar radiation pressure, and guidance and control of a solar sail spacecraft in interplanetary space. NASA also launched a solar sail spacecraft called NanoSail-D2 into a low Earth orbit in 2010. IKAROS and NanoSail-D2 are to be followed by several solar sail projects. The importance of solar sails is widely acknowledged, and solar sails are being as popular as ever.

This thesis deals with a spinning solar sail in interplanetary space. In general, spinning solar sails are considered to have a good prospect compared to three-axis stabilised solar sails. This is because the fact that spinning solar sails do not require such rigid structures as booms or masts leads to weigh reduction. This is a critical criterion for solar sails since a high sail area-to-mass ratio is necessary to use solar radiation pressure for propulsion.

In past Japanese deep space missions including IKAROS, it was shown that the spin-axis direction of a spinning spacecraft rotates around an equilibrium direction near the Sun direction due to the effect of solar radiation pressure. This phenomenon is called an “attitude drift motion”. It is known that this attitude motion can be controlled by the spin rate of the spacecraft. The solar radiation pressure force on the sail, hence the acceleration gained by the solar sail, is dependent on the attitude with respect to the Sun. The orbit of a spinning solar sail can be, therefore, controlled indirectly by the spin rate through the attitude drift motion. In this thesis, the attitude and orbit control of a spinning solar sail by the spin rate is proposed.

Spin rate control laws for optimal attitude and orbit control are determined. Analytical and numerical analyses are performed to solve optimal control problems for acceleration and deceleration maximisation, orbital elements optimisation, attitude control optimisation and circular orbit-to-circular orbit transfer optimisation. The significance of this thesis is that a pure under-actuated system is investigated. The six degrees of freedom of the attitude and orbital motions are controlled only by the spin rate. It provides ultimate redundancy and simplicity for a spinning solar sail because it enables the attitude and orbit control of the spacecraft provided that only the spin rate is controllable. The control strategy proposed in this thesis, therefore, greatly contributes to the guidance and control of future spinning solar sails.

Contents

Chapter 1

Introduction

1.1 Background

Solar sails are a form of spacecraft which deploys a large sail in space and uses solar radiation pressure for propulsion. They gain momentum by reflecting photons of which Sunlight is composed. The momentum that can be gained by a single photon is extremely small. A solar sail spacecraft must be light and deploy a large sail in order to be accelerated slowly but continuously by Sunlight. Solar sailing is considered as an ultimate propulsion system since it does not require any propellant.

The existence of light pressure was shown theoretically by the Scottish physicist James Clark Maxwell in 1873, and was proved experimentally by the Russian physicist Peter Lebedew in 1900 [1 ,2]. In 1921, the famous Russian rocket scientist Konstantin Tsiolkovsky was the first to write about propulsion using Sunlight. He proposed that it would be possible to propel with a large shining membrane of very thin film using solar radiation pressure [3]. Since then, solar sails have been studied by numerous researchers. Studies have demonstrated potential advantages and benefits of solar sailing. Solar sails have also appeared in science fiction novels. Notably the famous short story *The Wind from the Sun* published by Arthur C. Clarke in 1963 contributed to the spread of the idea of solar sailing. Solar sails were, however, not realised for a long period of time.

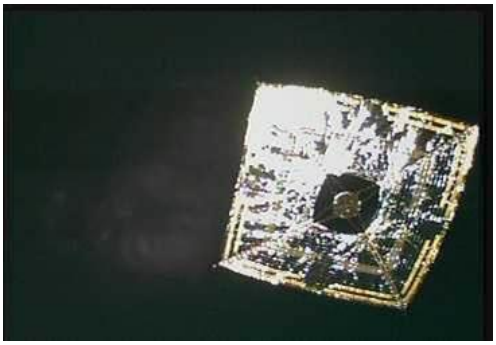

Fig. 1.1 Small Solar Power Sail Demonstrator IKAROS.

In 2010, the first solar sail spacecraft in the world has finally come true. The name of the spacecraft is IKAROS (Interplanetary Kite-craft Accelerated by Radiation Of the Sun), shown in Fig. 1.1 [4, 5]. It was developed by Japan Aerospace Exploration Agency (JAXA) and launched on 21 May 2010. IKAROS is a spinning solar sail, which is a spin-stabilised spacecraft, and deploys and stretches its sail using the centrifugal force due to spinning. The objective of IKAROS was to demonstrate various novel technologies regarding solar sailing: the deployment of a 200 m^2 sail, power generation with thin-film solar cells on the sail, measurement of acceleration due to solar radiation pressure, and guidance and control of a solar sail spacecraft in interplanetary space. IKAROS achieved the objective successfully and became the first solar sail spacecraft in the world. Fig. 1.1 is a real image taken in space with a separation camera [6].

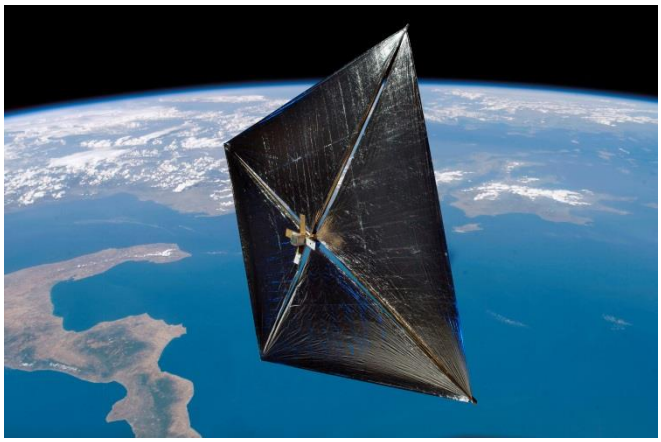

Fig. 1.2 NanoSail-D.

Whereas IKAROS is a spinning solar sail, another major type of solar sails is a three-axis stabilised solar sail, which is composed of booms or masts to deploy and stretch a sail. NanoSail-D2 shown in Fig. 1.2 was developed by NASA and launched on 20 November 2010 subsequently to the loss of NanoSail-D in 2008 due to a rocket malfunction [7]. It is a three-unit CubeSat with a mass of 4 kg. The main objective was to demonstrate and test the deorbiting capabilities of a sail as a drag augmentation device in a low Earth orbit. After more than 240 days in orbit, the spacecraft re-entered the Earth's atmosphere.

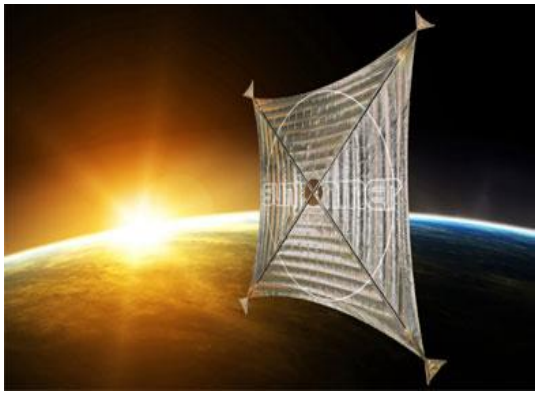

Fig. 1.3 Sunjammer.

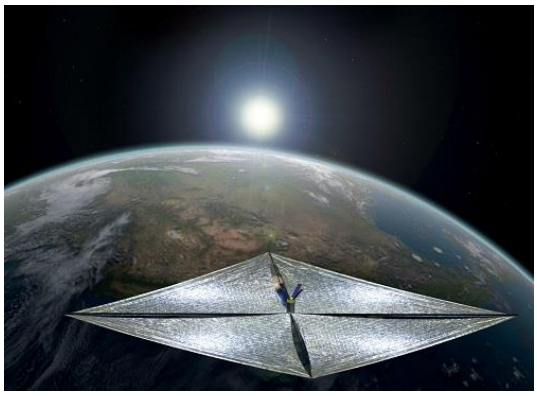

Fig. 1.4 LightSail-1.

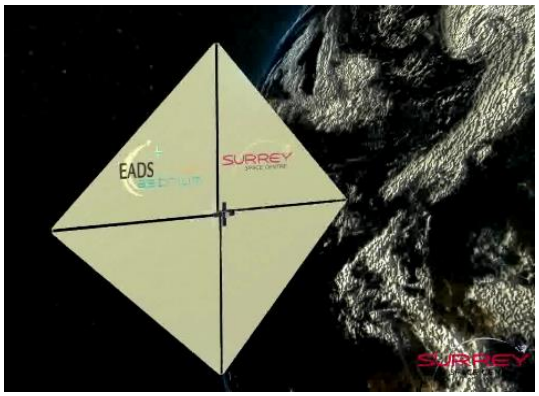

Fig.1.5 CubeSail.

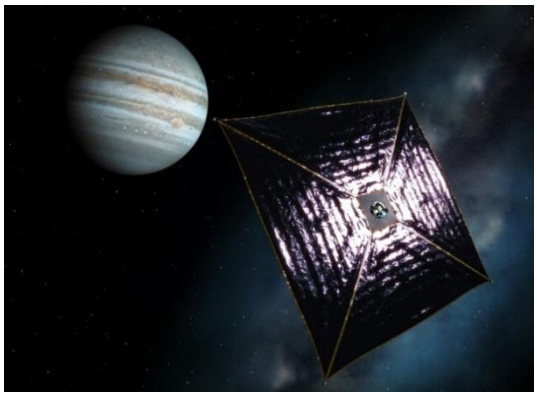

Fig. 1.6 Solar Power Sail.

In addition, there are several solar sail projects under consideration. Sunjammer in Fig. 1.3 is NASA's first solar sail to deep space [8]. It will demonstrate the deployment of a 1200 m^2 sail, the largest solar sail as of 2014, and test navigation capabilities. LightSail-1 in Fig. 1.4 is a solar sail developed by The Planetary Society [9]. It is a part of LightSail program to develop three separate solar sails over several years. The main goal of LightSail-1 is to fly in Earth orbit and demonstrate photon propulsion. The Surrey Space Centre in the United Kingdom are developing CubeSail, which is shown in Fig. 1.5, with a sail area of 25 m^2 to demonstrate photon propulsion and the deorbiting capabilities of a sail [10]. Moreover, a solar sail mission to explore Jovian Trojan asteroid is under consideration at JAXA to be launched in around 2020 [11]. A 3000 m^2 sail will majorly consist of thin-film solar cells in order to enable the spacecraft to generate sufficient power to drive an electric propulsion system at a distance of approximately 5 AU from the Sun. The importance of solar sails as various purposes is widely acknowledged, and solar sails are being as popular as ever.

1.2 Problem Statement

This thesis deals with a spinning solar sail in interplanetary space. In general, spinning solar sails are considered to have a good prospect compared to three-axis stabilised solar sails. This is because the fact that spinning solar sails do not require such rigid structures as booms or masts leads to weigh reduction. This is a critical criterion for solar sails since a high sail area-to-mass ratio is necessary to use solar radiation pressure for propulsion.

In past Japanese deep space missions including IKAROS, it was demonstrated that the spin-axis direction of a spinning spacecraft is capable of tracking the Sun direction automatically [12, 13]. The spin-axis direction rotates around an equilibrium direction near the Sun direction due to the effect of solar radiation pressure. This phenomenon is called an "attitude drift motion".

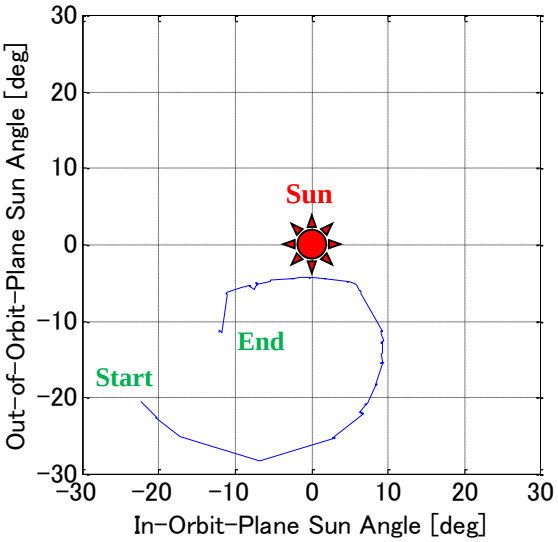

Fig. 1.7 Attitude Drift Motion of IKAROS.

Fig. 1.7 shows the attitude history of IKAROS for approximately 2 months. The spin-axis direction is seen from the Sun, which is at the origin, and the horizontal axis of the figure is on the orbit plane of IKAROS. As can be seen, the spin-axis direction rotates anti-clockwise although no active attitude control is performed in this period.

As explained in the next chapter, the attitude drift motion of a spinning solar sail is dependent on the proportion of a torque induced by solar radiation pressure and the angular momentum of the solar sail. It can be, therefore, controlled by the spin rate because the angular momentum varies according to the spin rate. Moreover, since the solar radiation pressure force on the sail, hence the acceleration gained by the spacecraft, is dependent on the attitude with respect to the Sun, the orbit of a spinning solar sail can be controlled indirectly by the spin rate through the attitude drift motion. This is an interesting and important characteristic of a spinning solar sail. In this thesis, the attitude and orbit control of a spinning solar sail by the spin rate is proposed.

A method to control the spin rate is not necessarily specified in this thesis. The most conventional way is to use chemical thrusters with propellant. This has been performed in operations of IKAROS. The use of "reflectivity control device" has also been demonstrated with IKAROS [14]. This is a device whose optical parameters can be changed electrically, and it can be used for attitude or spin rate control of a spacecraft by generating a torque using solar radiation pressure. It may also be possible to use vanes at tips of a sail. While several ideas can be conceived for spin rate control, the concept to perform attitude and orbit control by spin rate control is important in this thesis.

The significance of this research is that a pure under-actuated system is investigated. The six degrees of freedom of the attitude and orbital motions are controlled by single control input, which is the spin rate. In other words, the attitude and orbit of a spinning solar sail is controlled by a minimum control degree of freedom. Needless to say, it is superior to control the three degrees of freedom of attitude motion in terms of control efficiency for attitude and orbit control; however, it requires more number of control degree of freedom. The control strategy proposed in this thesis provides ultimate redundancy and simplicity for a spinning solar sail because it enables the guidance and control of the spacecraft provided that only the spin rate is controllable.

It is also possible to realise the attitude and orbit control using the attitude drift motion by generating a torque in a perpendicular direction to the spin axis of a spinning solar sail instead of by spin rate control. It is, however, known that the spin rate of a spinning solar sail may increase or decrease naturally due to the shape deformation of the sail [15]. It is, therefore, required that the spin rate is controllable in any case, and the single control input for the attitude and orbit control of a spinning solar sail must be the spin rate.

In previous work, it is shown that the orbit control by the spin rate is feasible to be applied in some cases [16, 17, 18]. It is, however, limited to very specific problems, such as the guidance and control of IKAROS to the sphere of influence of the Earth or Venus. On the other hand, the objective of this thesis is to determine spin rate control laws for more general problems of attitude and orbit control of a spinning solar sail. An approach taken in this thesis is to solve optimal control problems for several different purposes analytically, and to perform numerical analyses in order to prove the validity of the analytical derivation. The direct collocation with nonlinear programming method is used for the numerical analyses [19, 20].

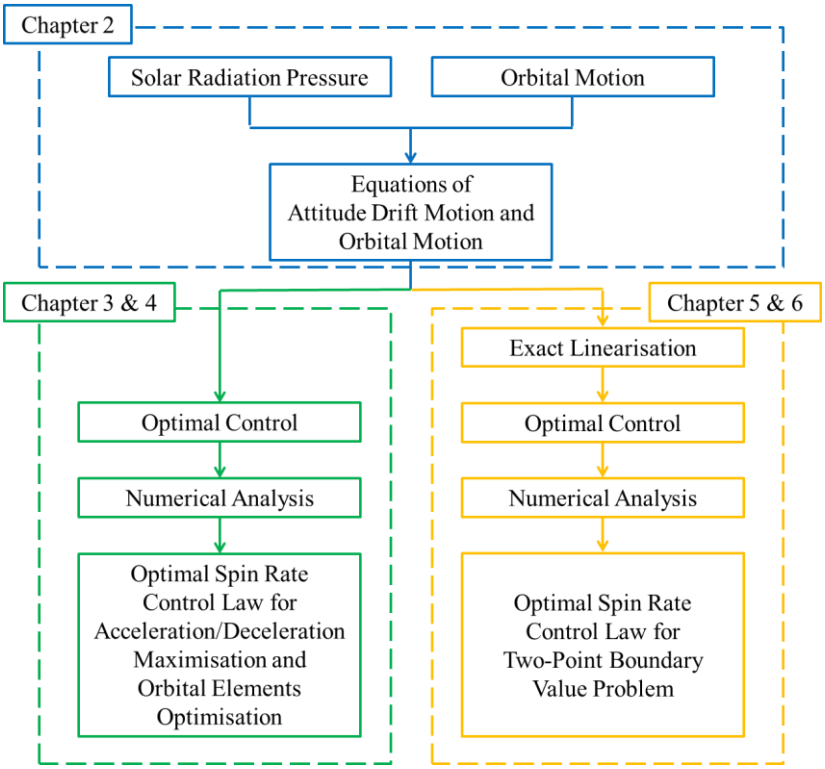

Fig. 1.8 Thesis Overview.

Figure 1.8 summarises the overview of this thesis. As shown in the figure, the work in this thesis is divided into the following chapters.

Chapter 2. Attitude and Orbit Dynamics Models

In this chapter, dynamics models that are used in this thesis are introduced, and equations of attitude and orbital motions are shown. With regard to the attitude motion of a spinning solar sail, equations of the attitude drift motion are derived to demonstrate the rotational motion of the spin-axis direction around an equilibrium direction. The equations show that the attitude drift motion can be controlled by the spin rate. The orbital motion of a spinning solar sail is calculated using the two-body problem in this thesis. Equations of orbital motion including solar radiation pressure are shown.

Chapter 3. Acceleration and Deceleration Manoeuvres

As the most fundamental orbit control manoeuvres, optimal spin rate control laws to accelerate and decelerate a spinning solar sail are derived by optimising the attitude drift motion. Optimal control problems are formulated with cost functions of solar radiation pressure acceleration to maximise the acceleration and deceleration in the transverse direction. Analytical derivations and numerical analyses prove that simple bang-bang control of the spin rate is optimal as acceleration and deceleration manoeuvres.

Chapter 4. Orbital Elements Optimisation

Orbital elements are optimised in this chapter. Optimal spin rate control laws for orbital inclination maximisation, orbital eccentricity maximisation, aphelion maximisation and perihelion minimisation are determined. In every problem, a locally optimal trajectory is determined by optimising the attitude drift motion analytically, and it is followed by a numerical optimisation to determine a globally optimal trajectory and to prove the validity of the analytical solution.

Chapter 5. Exact Linearisation of Bilinear System for Attitude Control Manoeuvres

In this chapter, nonlinear equations of the attitude drift motion are linearised using a method called “exact linearisation". It is a method to transform a nonlinear system into an equivalent linear system using a coordinate transformation and state feedback. The effectiveness of the exact linearisation is demonstrated by formulating an optimal control problem of attitude control manoeuvres that is analytically solvable. Since the attitude drift motion can be controlled by the spin rate, attitude control can be performed by controlling the spin rate and using the attitude drift motion. An optimal spin rate control law to perform attitude control is determined analytically.

Chapter 6. Circular Orbit-to-Circular Orbit Transfer Optimisation

The exact linearisation is used to linearise equations of the attitude drift motion, and its effectiveness is proved with example attitude control manoeuvres in the previous chapter. In this chapter, on the other hand, orbit control of a spinning solar sail using the exact linearisation is investigated. Exactly linearised equations of the attitude drift motion are combined with the equations of orbital motion. The attitude and orbital motions are dealt with analytically simultaneously, and globally optimal trajectories for a circular orbit-to-circular orbit transfer are determined. It is assumed that a spinning solar sail is initially in a circular orbit in the ecliptic plane with a radius of 1 AU, and it is transferred to another circular orbit with a larger radius.

Chapter 2

Attitude and Orbit Dynamics Models

2.1 Attitude Drift Motion

2.1.1 Introduction

The attitude drift motion was used for the first time with Asteroid Explorer Hayabusa (MUSES-C) [21]. Hayabusa was developed and launched by JAXA in 2003 to demonstrate novel technologies for asteroid exploration and sample return. It accomplished its objectives and successfully returned to the Earth with dust grain samples from the asteroid in 2010 [22, 23]. During the journey of Hayabusa, one of difficult moments was when it lost most of its fuel for chemical thrusters due to a leak problem [24]. Since the spacecraft was required to be pointing to the Sun direction for power generation with solar array panels, Xe gas for an electric propulsion system was used as cold gas thrusters instead. It was, however, estimated that the amount of Xe gas required would exceed the residual if a conventional control scheme was adopted.

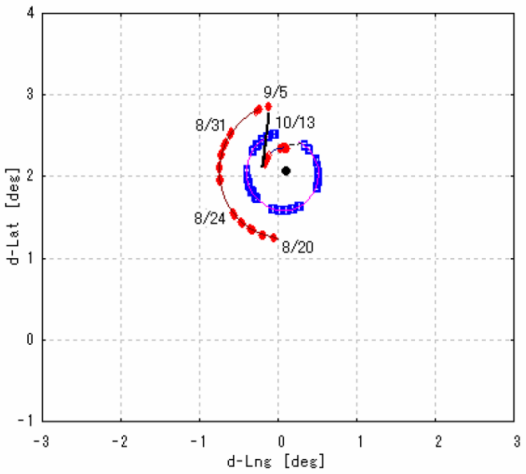

Fig. 2.1 Attitude Drift Motion of Hayabusa.

The project team decided to take advantage of solar radiation pressure to control the attitude motion of the spacecraft, and proved that the spin-axis direction of the spacecraft can track the Sun direction automatically. The flight data is shown in Fig. 2.1. This invention was crucial for Hayabusa. It was possible to track the Sun direction with no fuel use using the attitude drift motion, and it contributed to Xe gas saving for the return to the Earth.

Moreover, the attitude drift motion was also observed with IKAROS as introduced in the previous chapter. The attitude drift motion of IKAROS was slightly different from that of Hayabusa due to the shape deformation of the sail. In this thesis, the attitude drift motion with a completely flat sail, which is similar to that of Hayabusa, is considered. The dynamics of the attitude drift motion is introduced in this section.

2.1.2 Coordinate Systems

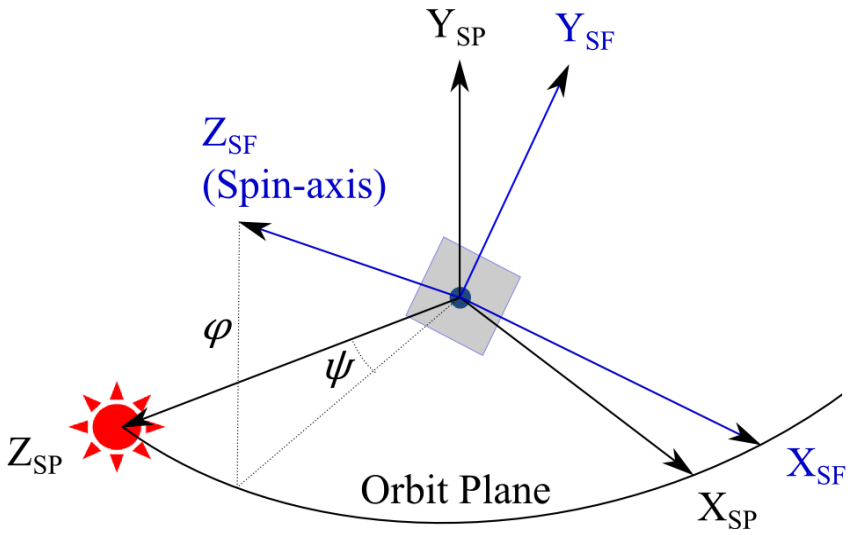

Fig. 2.2 Sun-Pointing and Spin-Free Coordinate Systems.

Two coordinate systems used to express the attitude motion are introduced as shown in Fig. 2.2. Firstly, the Sun-pointing coordinate system is defined. The origin is at the centre of mass of the spacecraft. The z-axis is in the Sun direction, and the y-axis is perpendicular to the orbit plane of the spacecraft while the x-axis is defined to form a right-handed coordinate system.

Secondly, the spin-free coordinate system is introduced. While the attitude of a spinning spacecraft is not required to be described with its three axes, its spin-axis direction is important. In the spin-free coordinate system, the origin is defined to be the centre of mass of the spacecraft. A coordinate transformation is executed with angles φ and ψ from the Sun-pointing coordinate system so that the z-axis coincides with the spin-axis direction. These angles are called out-of-orbit-plane Sun angle and in-orbit-plane Sun angle. In this paper, the attitude motion of a spacecraft is written in the spin-free coordinate system and expressed in terms of φ and ψ.

2.1.3 Equations of Attitude Drift Motion

Equations of the attitude drift motion are derived in this subsection. The equations in this subsection are written in the spin-free coordinate system.

If a solar sail spacecraft has a completely flat sail, the solar radiation pressure force experienced by the sail, $\boldsymbol{F}_{SRP}$, can be expressed with Eq. (2.1).

$$\boldsymbol{F}_{SRP} = -\frac{P_0 A}{c}\left(\frac{R_0}{r}\right)^2 (\boldsymbol{s}\cdot\boldsymbol{n})\left\{\left(C_{abs}+C_{dif}\right)\boldsymbol{s}+\left(\frac{2}{3}C_{dif}+2C_{spe}(\boldsymbol{s}\cdot\boldsymbol{n})\right)\boldsymbol{n}\right\} \tag{2.1}$$

P_0 is the solar constant; A is the area of the sail; c is the speed of light; R_0 is the mean distance between the Sun and the Earth (i.e. 1 AU); r is the distance between the Sun and the spacecraft; $\boldsymbol{s}$ is the spacecraft-to-Sun vector; $\boldsymbol{n}$ is a normal vector to the sail; and C_{spe}, C_{dif} and C_{abs} are specular reflectivity, diffuse reflectivity and absorptivity respectively.

The solar radiation pressure torque, which causes the attitude drift motion, is based on an idea that there is an offset between the centre of mass of the solar sail spacecraft and the centre of the solar radiation pressure on the sail. Given that the sail is flat, the centre of the solar radiation pressure can be considered as the centroid of the sail. Thus the centre of the solar radiation pressure is on the spin axis, and the lever arm vector, $\boldsymbol{L}$, is assumed to be parallel to the spin axis.

$$\boldsymbol{L} = L\begin{pmatrix}0\\0\\1\end{pmatrix} \tag{2.2}$$

where L is the distance between the centre of mass of the spacecraft and the centre of the solar radiation pressure. The resulting solar radiation pressure torque, $\boldsymbol{T}_{SRP}$, is determined with Eq. (2.3).

$$\boldsymbol{T}_{SRP} = \boldsymbol{L}\times\boldsymbol{F}_{SRP} \tag{2.3}$$

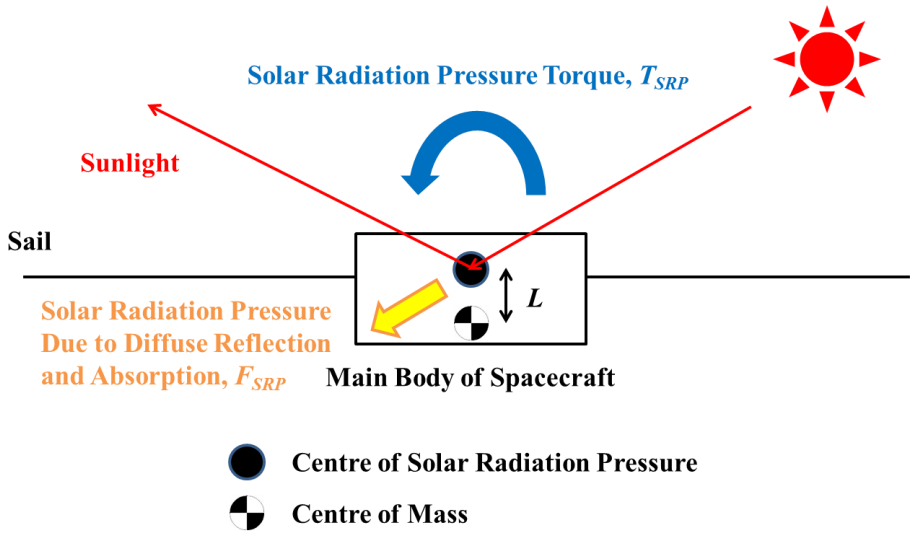

Fig. 2.3 Solar Radiation Pressure Torque.

Figure 2.3 represents the idea of the solar radiation pressure torque due to the solar radiation pressure force. Using Eqs. (2.1), (2.2) and (2.3), the solar radiation pressure torque can be written with Eq. (2.4) using the out-of-orbit-plane and in-orbit-plane Sun angles, φ and ψ

$$\boldsymbol{T}_{SRP} = \frac{P_0 AL}{c}\left(\frac{R_0}{r}\right)^2 \left(C_{abs} + C_{dif}\right)\begin{pmatrix} -sin\varphi\ cos\varphi\ cos^2\psi \\ cos\varphi\ sin\psi\ cos\psi \\ 0 \end{pmatrix} \tag{2.4}$$

Eq. (2.5) shows the Euler's equation in the spin-free coordinate system.

$$\dot{\boldsymbol{H}} + \tilde{\boldsymbol{\omega}} \times \boldsymbol{H} = \boldsymbol{T}_{SRP} \tag{2.5}$$

$\boldsymbol{H}$ is the angular momentum vector of the spacecraft, and $\tilde{\boldsymbol{\omega}}$ is the angular velocity vector of the spin-free coordinate system with respect to the inertial frame. Their components are as shown in Eq. (2.6).

$$H = \begin{pmatrix} I_T\omega_x \\ I_T\omega_y \\ I_S\Omega \end{pmatrix}, \tilde{\omega} = \begin{pmatrix} \omega_x \\ \omega_y \\ 0 \end{pmatrix} \tag{2.6}$$

I_S is the moment of inertia around the spin axis, I_T is the moment of inertia around an axis perpendicular to the spin axis, and Ω is the spin rate. Substituting Eqs. (2.4) and (2.6) into Eq. (2.5), the x and y components of Eq. (2.5) can be written as follows:

$$\begin{aligned} \dot{\omega}_x + \Omega_n\omega_y &= -p\ sin\varphi\ cos\varphi\ cos^2\psi \\ \dot{\omega}_y - \Omega_n\omega_x &= p\ cos\varphi\ sin\psi\ cos\psi \end{aligned} \tag{2.7}$$

Ω_n and p are parameters introduced for simplification and defined as in Eq. (2.8).

$$\Omega_n = \frac{I_S}{I_T}\Omega, p = \frac{P_0 AL}{cI_T}\left(\frac{R_0}{r}\right)^2 \left(C_{abs} + C_{dif}\right) \tag{2.8}$$

p is named as "solar radiation pressure parameter". Using the relationship between the Sun-pointing and spin-free coordinate systems, Eq. (2.9) can be derived.

$$\omega_x = -\dot{\varphi}, \omega_y = \left(\dot{\psi} + \omega_s\right)cos\varphi \tag{2.9}$$

ω_s is the angular velocity of the spacecraft in the inertial frame. Substituting Eq. (2.9) into Eq. (2.7), Eq. (2.10) can be derived. It is based on an assumption that φ and ψ are small enough, and the trigonometric functions are approximated with their first term of the Taylor series.

$$\begin{aligned} \ddot{\varphi} - \Omega_n\dot{\psi} &= p\varphi + \Omega_n\omega_s \\ \ddot{\psi} + \Omega_n\dot{\varphi} &= p\psi \end{aligned} \tag{2.10}$$

Transforming Eq. (2.10) into the form shown in Eq. (2.11) and using the relationship in Eq. (2.12), the characteristic equation and its solution can be written as in Eq. (2.13).

$$\begin{aligned} \varphi^{(4)} + \left({\Omega_n}^2 - 2p\right)\varphi^{(2)} + p^2\varphi &= -\Omega_n p\omega_s \\ \psi^{(4)} + \left({\Omega_n}^2 - 2p\right)\psi^{(2)} + p^2\psi &= 0 \end{aligned} \tag{2.11}$$

$$\frac{p}{{\Omega_n}^2} \ll 1 \tag{2.12}$$

$$\lambda^4 + \left({\Omega_n}^2 - 2p\right)\lambda^{(2)} + p^2 = 0$$
$$\lambda \approx \pm i\Omega_n, \pm i\frac{p}{\Omega_n} \tag{2.13}$$

Therefore, the attitude drift motion can be expressed with Eq. (2.14) where A, B, C and D are constants of integration.

$$\varphi = A\cos\left(\frac{p}{\Omega_n}t + B\right) + C\cos(\Omega_n t + D) - \frac{\Omega_n}{p}\omega_s$$
$$\psi = -A\sin\left(\frac{p}{\Omega_n}t + B\right) - C\sin(\Omega_n t + D) \tag{2.14}$$

The first and second terms represent the precession and nutation of the spin axis respectively, which result in a rotational motion around an equilibrium direction of $\left(-\frac{\Omega_n}{p}\omega_s, 0\right)$.

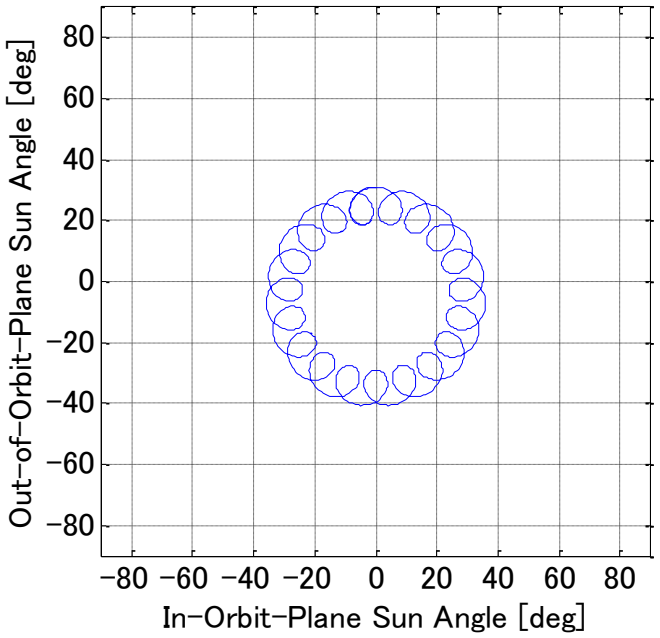

Fig. 2.4 Precession and Nutation.

Figure 2.4 shows an example of the attitude drift motion in Eq. (2.14). The larger and slower rotational motion corresponds to the precession whereas the smaller and faster motion is the nutation. The constants of integration are given arbitrarily for ease of demonstration. Although the nutation is greatly exaggerated in the figure, it is in general negligible compared to the precession because its amplitude is much smaller than that of the precession. In this paper, it is assumed that the spacecraft is always in pure rotation, and only the precession is taken into account as shown in Eq. (2.15).

$$\varphi = A\cos\left(\frac{p}{\Omega_n}t + B\right) - \frac{\Omega_n}{p}\omega_s$$
$$\psi = -A\sin\left(\frac{p}{\Omega_n}t + B\right) \tag{2.15}$$

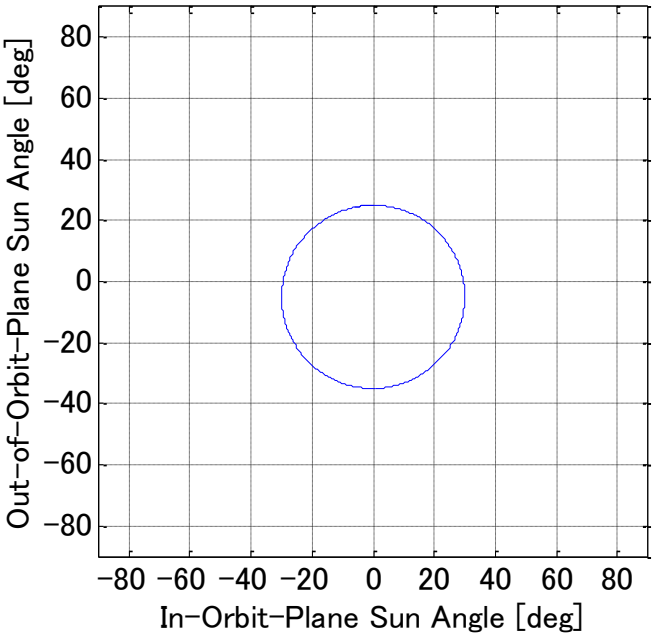

Fig. 2.5 Precession.

Eq. (2.15) results in a simple rotation of the spin axis around an equilibrium direction, as shown in Fig. 2.5. As can be seen in the equation, the period of the attitude drift motion, $\frac{p}{\Omega_n}$, and the equilibrium direction, $\left(-\frac{\Omega_n}{p}\omega_s, 0\right)$, are dependent on the spin rate, Ω_n. The attitude drift motion can be, therefore, controlled by the spin rate. This characteristic enables indirect attitude and orbit control of a spinning solar sail by the spin rate through the attitude drift motion.

The period and the equilibrium direction are, nevertheless, also a function of the solar radiation pressure parameter, p. This is because, as introduced in Chapter 1, the attitude drift motion is determined with the proportion of the solar radiation pressure torque and the angular momentum of the solar sail. This characteristic is shown mathematically in Eq. (2.15). It is, therefore, possible to control the attitude drift motion by controlling the centre of mass of the spacecraft with an actuator, for example, since the solar radiation pressure parameter, p, is a function of the distance between the centre of mass and the centre of solar radiation pressure, L. This corresponds to controlling the magnitude of the solar radiation pressure torque, and it is totally equivalent to the angular momentum control with the spin rate in terms of the control of the attitude drift motion. In this thesis, it is suggested to perform the attitude and orbit control through the attitude drift motion by spin rate control because it is most likely to be difficult to move the centre of mass of a spacecraft sufficiently for such a purpose. Additionally, the spin rate is required to be controllable as the spin rate may increase or decrease naturally due to the shape deformation of the sail. The control method proposed in this thesis, however, does not have to be performed with spin rate control, and it has flexibility.

Differential equations of the attitude drift motion can be derived as follows from Eq. (2.15):

$$\dot{\varphi} = \omega\psi$$
$$\dot{\psi} = -\omega\varphi - \omega_s \tag{2.16}$$

where

$$\omega = \frac{p}{\Omega_n} \tag{2.17}$$

2.2 Orbital Motion

2.2.1 Coordinate System

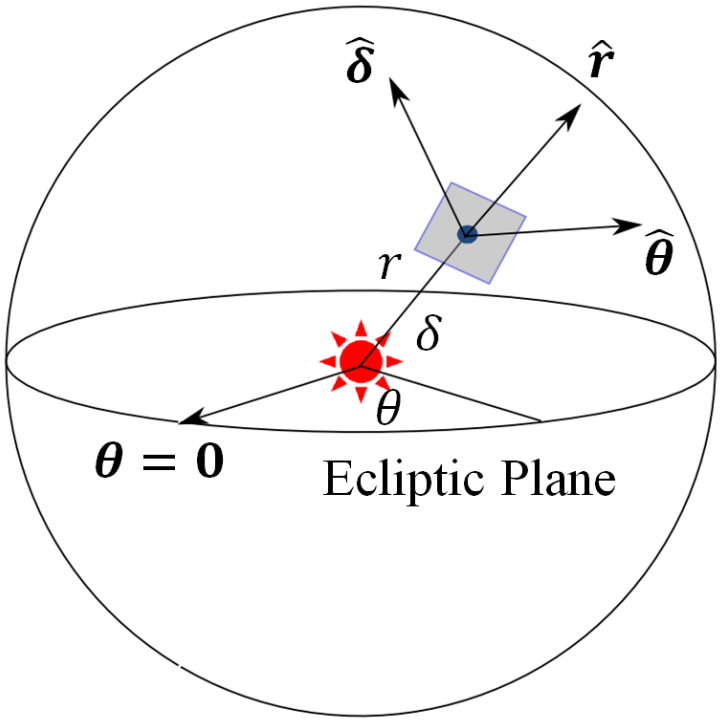

Fig. 2.6 Spherical Polar Coordinate System.

The spherical polar coordinate system shown in Fig. 2.6 is used to express the three-dimensional orbital motion of a spinning solar sail in this thesis. The origin is defined to be the centre of mass of the Sun, and the position of the spacecraft is expressed with the radial distance r, the azimuth angle θ and the elevation angle δ.

2.2.2 Equations of Orbital Motion

In this thesis, the orbital motion of a spinning solar sail is calculated using the Sun-spacecraft two-body problem. The equations of motion in the spherical polar coordinate system, can be written as follows:

$$\begin{aligned}\ddot{r} &= -\frac{\mu}{r^2} + r\dot{\delta}^2 + r\dot{\theta}^2\cos^2\delta + a_r \\ \ddot{\theta} &= 2\dot{\theta}\dot{\delta}tan\delta - \frac{2}{r}\dot{r}\dot{\theta} + \frac{a_\theta}{rcos\delta} \\ \ddot{\delta} &= -\dot{\theta}^2 sin\delta cos\delta - \frac{2}{r}\dot{r}\dot{\delta} + \frac{a_\delta}{r}\end{aligned} \tag{2.18}$$

where μ is the standard gravitational parameter of the Sun. The terms a_r, a_θ and a_δ denote the solar radiation pressure acceleration experienced by a solar sail spacecraft. They are a function of the attitude of the spacecraft with respect to the Sun and are expressed using the out-of-orbit-plane and in-orbit-plane Sun angles.

$$\begin{aligned}a_r &= \frac{P_0 A}{mc}\left(\frac{R_0}{r}\right)^2\left(2C_{spe}cos^3\varphi cos^3\psi + \frac{2}{3}C_{dif}cos^2\varphi cos^2\psi + \left(C_{abs}+C_{dif}\right)cos\varphi cos\psi\right) \\ a_\theta &= \frac{P_0 A}{mc}\left(\frac{R_0}{r}\right)^2\left(2C_{spe}sin\psi cos^3\varphi cos^2\psi + \frac{2}{3}C_{dif}sin\psi cos^2\varphi cos\psi\right) \\ a_\delta &= \frac{P_0 A}{mc}\left(\frac{R_0}{r}\right)^2\left(-2C_{spe}sin\varphi cos^2\varphi cos^2\psi - \frac{2}{3}C_{dif}sin\varphi cos\varphi cos\psi\right)\end{aligned} \tag{2.19}$$

where m is the mass of the spacecraft.

The values of constants, such as the optical parameters and the moment of inertia, used throughout this thesis are based on the design of IKAROS, which is summarised in Appendix A. Only exceptions are the sail area and mass. The performance of a solar sail is critically determined with the sail area-to-mass ratio since the magnitude of the solar radiation pressure acceleration is dominated with this ratio as shown in Eq. (2.19). This is a crucial design parameter, and the performance of a solar sail is generally evaluated with a parameter called "characteristic acceleration" introduced in Eq. (2.20).

$$a_0 = \frac{P_0 A}{mc}\left(2C_{spe} + \frac{5}{3}C_{dif} + C_{abs}\right) \tag{2.20}$$

The characteristic acceleration denotes the solar radiation pressure acceleration experienced by a solar sail spacecraft when facing the Sun at the distance of 1 AU from the Sun. In this thesis, the characteristic acceleration of 1 mm/s^2 is assumed for orbital motion calculations unless it is noted. This is because the characteristic acceleration of IKAROS is 6.08×10^{-3} mm/s^2, which is too low for orbit control using the solar radiation pressure. In other words, the performance of IKAROS as a solar sail is not high because it was launched as a demonstration spacecraft to prove various new technologies required for solar sails. In fact, although IKAROS demonstrated photon propulsion using solar radiation pressure and has become the world's first solar sail, orbit control using solar radiation pressure has been limited.

Chapter 3

Acceleration and Deceleration Manoeuvres

Since the work in this chapter is to be published as a peer-reviewed paper, it is deleted in this abridged version of thesis.

Chapter 4

Orbital Elements Optimisation

Since the work in this chapter is to be published as a peer-reviewed paper, it is deleted in this abridged version of thesis.

Chapter 5

Exact Linearisation of Bilinear System for Attitude Control Manoeuvres

5.1 Introduction

In previous chapters, the orbit control of a spinning solar sail is investigated, and it is determined that the bang-bang control of the spin rate is an optimal solution of several orbit control problems. It is, however, difficult to perform sophisticated control that satisfies initial and final conditions with the bang-bang control of the spin rate. This is because the maximum and minimum spin rate is switched over to one after the other purely according to a switching function. In this chapter, linearisation of the equations of the attitude drift motion is performed using a method called “exact linearisation" in order to solve a two-point boundary value problem with initial and final conditions to be satisfied. The effectiveness of the method is examined by applying it to example attitude control manoeuvres.

As it is shown throughout this thesis, the attitude drift motion of a spinning solar sail can be controlled by the spin rate. In other words, attitude control can be performed by controlling the spin rate and using the attitude drift motion. An optimal spin rate control law to perform attitude control is determined analytically in this chapter [27].

5.2 Exact Linearisation of Attitude Drift Motion

The equations of the attitude drift motion are shown in Eq. (5.1).

$$\begin{aligned} \dot{\varphi} &= \omega\psi \\ \dot{\psi} &= -\omega\varphi - n \end{aligned} \tag{5.1}$$

In Eq. (5.1), the out-of-orbit-plane and in-orbit-plane Sun angles, ϕ and ψ, are state variables while ω is control input since it is a function of the spin rate. Hence this is a type of nonlinear systems

called a bilinear system. It is defined as a class of nonlinear systems, in which nonlinear terms are constructed by a multiplication of state variables and control input.

In general, it is impossible to solve an optimal control problem analytically for nonlinear systems except for the simplest problems. An approach to be taken in such a case is a method called exact linearisation [28]. It is a technique to transform a nonlinear system into an equivalent linear system using a coordinate transformation and state feedback. For example, an approximation using the first-order Taylor expansion around a steady state is effective only in a small region; the accuracy degrades as it leaves from the steady state. There is, however, no approximation in the exact linearisation, and nonlinear characteristics of a nonlinear system are rigorously preserved. An optimal control problem for a nonlinear system becomes analytically solvable by linearising the system.

A general nonlinear system is written in Eq. (5.2).

$$\frac{dx}{dt} = f(x) + g(x)u \tag{5.2}$$

where x is an n-dimensional state vector, u is scalar control input, and $f(x)$ and $g(x)$ are functions of the state vector. It is known that the following necessary and sufficient conditions must be satisfied for such a nonlinear system to be exactly linearised [29, 30, 31].

1. $\{ad_f^0 g, ad_f^1 g, ad_f^2 g, \cdots, ad_f^{n-1} g\}(x)$ is linearly independent for all x
2. $\{ad_f^0 g, ad_f^1 g, ad_f^2 g, \cdots, ad_f^{n-2} g\}(x)$ is involutive

where

$$ad_f^0 g = g(x) \tag{5.3}$$

$$ad_f^{i+1} g = [f, ad_f^i g] \tag{5.4}$$

$$[f, g] = \frac{\partial g}{\partial x} f(x) - \frac{\partial f}{\partial x} g(x) \tag{5.5}$$

$[f, g]$ is the Lie bracket which functions as the commutator of vector fields. The equations below shows that the equations of the attitude drift motion meet the two conditions above.

$$\frac{d}{dt}\begin{pmatrix}\phi\\ \psi\end{pmatrix} = \begin{pmatrix}0\\ -n\end{pmatrix} + \begin{pmatrix}\psi\\ -\phi\end{pmatrix}\omega \tag{5.6}$$

Eq. (5.6) shows the equations of the attitude drift motion in a different form.

$$ad_f^0 g = g(x) = \begin{pmatrix}\psi\\ -\phi\end{pmatrix} \tag{5.7}$$

$$ad_f^1 g = [f, g](x) = \frac{\partial g}{\partial x} f(x) - \frac{\partial f}{\partial x} g(x) = \begin{pmatrix}-n\\ 0\end{pmatrix} \tag{5.8}$$

From Eqs. (5.7) and (5.8), it is confirmed that $\{ad_f^0 g, ad_f^1 g\}(x)$ is linearly independent.

$$[ad_f^0 g, ad_f^0 g](x) = 0 \tag{5.9}$$

Moreover, Eq. (5.9) proves that $\left[ad_f^0 g, ad_f^0 g\right](x)$ is involutive. Thus the two necessary and sufficient conditions are satisfied, and the equations of the attitude drift motion can be exactly linearised.

Now the coordinate transformation and state feedback required for the linearisation are determined using the Lie derivative.

$$L_{ad_f^0 g}\Phi(x) = \begin{pmatrix}\frac{\partial\Phi}{\partial\phi} & \frac{\partial\Phi}{\partial\psi}\end{pmatrix}\begin{pmatrix}\psi\\-\phi\end{pmatrix} = \frac{\partial\Phi}{\partial\phi}\psi - \frac{\partial\Phi}{\partial\psi}\phi = 0 \tag{5.10}$$

$$L_{ad_f^1 g}\Phi(x) = \begin{pmatrix}\frac{\partial\Phi}{\partial\phi} & \frac{\partial\Phi}{\partial\psi}\end{pmatrix}\begin{pmatrix}-n\\0\end{pmatrix} = -\frac{\partial\Phi}{\partial\phi}n \neq 0 \tag{5.11}$$

$\Phi(x)$ must satisfy Eqs. (5.10) and (5.11). A solution can be chosen as in Eq. (5.12).

$$\Phi = \phi^2 + \psi^2 \tag{5.12}$$

Since

$$\frac{\partial\Phi}{\partial\phi} = 2\phi \tag{5.13}$$

$$\frac{\partial\Phi}{\partial\psi} = 2\psi \tag{5.14}$$

Eq. (5.12) satisfies Eqs. (5.10) and (5.11). The coordinate transformation and state feedback are, therefore, determined as follows:

$$\begin{pmatrix}\xi_1\\\xi_2\end{pmatrix} = \begin{pmatrix}\Phi(x)\\L_f\Phi(x)\end{pmatrix} = \begin{pmatrix}\phi^2+\psi^2\\-2n\psi\end{pmatrix} \tag{5.15}$$

$$\omega = \frac{-L_f^2\Phi(x)+\omega'}{L_g L_f^1\Phi(x)} = -\frac{2n^2+\omega'}{2n\phi} \tag{5.16}$$

where

$$L_f\Phi(x) = \frac{\partial\Phi}{\partial x}f(x)\begin{pmatrix}2\phi & 2\psi\end{pmatrix}\begin{pmatrix}0\\-n\end{pmatrix} = -2n\psi \tag{5.17}$$

$$L_f^2\Phi(x) = L_f\{L_f\Phi(x)\} = \begin{pmatrix}0 & -2n\end{pmatrix}\begin{pmatrix}0\\-n\end{pmatrix} = 2n^2 \tag{5.18}$$

$$L_g L_f\Phi(x) = \begin{pmatrix}0 & -2n\end{pmatrix}\begin{pmatrix}\psi\\-\phi\end{pmatrix} = 2n\phi \tag{5.19}$$

Finally, the equations of the attitude drift motion can be exactly linearised using Eqs. (5.15) and (5.16).

$$\begin{aligned}\dot{\xi}_1 &= \xi_2\\ \dot{\xi}_2 &= \omega'\end{aligned} \tag{5.20}$$

ξ_1 and ξ_2 are new state variables, and ω' is new control input. As can be seen, the bilinear system in Eq. (5.1) is transformed into a simple linear system. Hence it enables an optical control problem that is analytically solvable to be formulated.

A time derivative of ω' is taken, and a linear system to be controlled is as follows.

$$\begin{aligned} \dot{\xi}_1 &= \xi_2 \\ \dot{\xi}_2 &= \xi_3 \\ \dot{\xi}_3 &= \omega'' \end{aligned} \tag{5.21}$$

where

$$\begin{pmatrix} \xi_1 \\ \xi_2 \\ \xi_3 \end{pmatrix} = \begin{pmatrix} \varphi^2 + \psi^2 \\ -2n\psi \\ 2n^2 + 2n\omega\varphi \end{pmatrix} \tag{5.22}$$

In Eq (5.21), ω'' is to be control input. It is essentially the angular acceleration of the in-orbit-plane Sun angle since $\omega'' = -2n\ddot{\psi}$.

5.3 Analytical Derivation

In this section, Eq. (5.21) is used instead of Eq. (5.1) as the equations of the attitude drift motion. An optimal control problem is formulated for attitude control manoeuvres and the effectiveness of the exact linearisation is shown.

The orbital motion is neglected in this chapter because it is focused on the attitude control. An optimal control problem is solved analytically using the Pontryagin's minimum principle.

$$J = \frac{1}{2}\int \omega''^2 \, dt \tag{5.23}$$

The cost function is defined as in Eq. (5.23). With this cost function, since ω'' is the angular acceleration of the in-orbit-plane Sun angle, $\ddot{\psi}^2$ will be minimised. This is an important factor since a general spacecraft generates electricity with solar cells, and it is required that the attitude of the spacecraft is pointing near to the Sun direction. By using the exact linearisation, such an optimal control problem can be solved analytically and rigorously. It would not be possible to solve the same problem analytically using the original bilinear system in Eq. (5.1). This is a powerful effectiveness of the exact linearisation. In addition, ω'' is a function of the change in the spin rate, $\dot{\omega}$, as shown below.

$$\omega'' = \dot{\omega}' = -2n\ddot{\psi} = 2n(\dot{\omega}\varphi + \omega\dot{\varphi}) = 2n(\dot{\omega}\varphi + \omega^2\psi) \approx 2n\dot{\omega}\varphi \tag{5.24}$$

The second term in the equation is neglected assuming a relationship of $\dot{\omega}\varphi \gg \omega^2\psi$ is likely to hold true. Hence it may contribute to the minimisation of the spin rate change to minimise the cost function in Eq. (5.23).

$$H = \frac{1}{2}\omega''^2 + +\lambda_{\xi_1}\xi_2 + \lambda_{\xi_2}\xi_3 + \lambda_{\xi_3}\omega'' \tag{5.25}$$

The Hamiltonian is defined in Eq. (5.25) using the co-state variables, λ_{ξ_1}, λ_{ξ_2} and λ_{ξ_3}. The optimal control input can be, therefore, derived as follows:

$$\frac{\partial H}{\partial \omega''} = \omega'' + \lambda_{\xi_3} = 0$$
$$\omega'' = -\lambda_{\xi_3} \tag{5.26}$$

The differential equations of the co-state variables are shown in Eq. (5.27) using Eqs. (5.21) and (5.26).

$$\begin{aligned}
\dot{\xi_1} &= \xi_2 \\
\dot{\xi_2} &= \xi_3 \\
\dot{\xi_3} &= -\lambda_{\xi_3} \\
\dot{\lambda_{\xi_1}} &= 0 \\
\dot{\lambda_{\xi_2}} &= -\lambda_{\xi_1} \\
\dot{\lambda_{\xi_3}} &= -\lambda_{\xi_2}
\end{aligned} \tag{5.27}$$

Eq. (5.27) can be solved analytically as follows:

$$\begin{aligned}
\xi_1 &= -\frac{1}{120} C_{\lambda_{\xi_1}} t^5 + \frac{1}{24} C_{\lambda_{\xi_2}} t^4 - \frac{1}{6} C_{\lambda_{\xi_3}} t^3 + \frac{1}{2} \xi_3(t_0) t^2 + \xi_2(t_0) t + \xi_1(t_0) \\
\xi_2 &= -\frac{1}{24} C_{\lambda_{\xi_1}} t^4 + \frac{1}{6} C_{\lambda_{\xi_2}} t^3 - \frac{1}{2} C_{\lambda_{\xi_3}} t^2 + \xi_3(t_0) t + \xi_2(t_0) \\
\xi_3 &= -\frac{1}{6} C_{\lambda_{\xi_1}} t^3 + \frac{1}{2} C_{\lambda_{\xi_2}} t^2 - C_{\lambda_{\xi_3}} t + \xi_3(t_0) \\
\lambda_{\xi_1} &= C_{\lambda_{\xi_1}} \\
\lambda_{\xi_2} &= -C_{\lambda_{\xi_1}} t + C_{\lambda_{\xi_2}} \\
\lambda_{\xi_3} &= \frac{1}{2} C_{\lambda_{\xi_1}} t^2 - C_{\lambda_{\xi_2}} t + C_{\lambda_{\xi_3}}
\end{aligned} \tag{5.28}$$

where $C_{\lambda_{\xi_1}}$, $C_{\lambda_{\xi_2}}$ and $C_{\lambda_{\xi_3}}$ are constants of integration, and $\xi_1(t_0)$, $\xi_2(t_0)$ and $\xi_3(t_0)$ are initial values of ξ_1, ξ_2 and ξ_3 at time t_0. The optimal control input is, therefore, derived as in Eq. (5.29)

$$\omega'' = -\frac{1}{2} C_{\lambda_{\xi_1}} t^2 + C_{\lambda_{\xi_2}} t - C_{\lambda_{\xi_3}} \tag{5.29}$$

To perform attitude control with specified initial and final conditions, final state constraints must be imposed as shown in Eq. (5.30).

$$\Phi\left[\boldsymbol{\xi}(t_f), t_f\right] = \mathbf{0} \tag{5.30}$$

The co-state variables at the final time are also defined in Eq. (5.31) using an undetermined multiplier vector, $\boldsymbol{\nu}$.

$$\boldsymbol{\lambda}^{\boldsymbol{T}}(t_f) = \left[\boldsymbol{\nu}^{\boldsymbol{T}} \frac{\partial \boldsymbol{\Phi}}{\partial \boldsymbol{\xi}}\right]_{\boldsymbol{t=t_f}} \tag{5.31}$$

Using Eqs. (5.30) and (5.31), the constants of integration in Eqs. (5.28) and (5.29) can be written in terms of ν_1, ν_2 and ν_3.

$$\begin{aligned}
\lambda_{\xi_1}(t_f) &= C_{\lambda_{\xi_1}} = \nu_1 \\
\lambda_{\xi_2}(t_f) &= -C_{\lambda_{\xi_1}} t_f + C_{\lambda_{\xi_2}} = \nu_2 \\
\lambda_{\xi_3}(t_f) &= \frac{1}{2} C_{\lambda_{\xi_1}} t_f^2 - C_{\lambda_{\xi_2}} t_f + C_{\lambda_{\xi_3}} = \nu_3
\end{aligned} \tag{5.32}$$

Substituting Eq. (5.32) into the first three lines in Eq. (5.28), the equations can be solved as simultaneous equations in terms of the undetermined multipliers.

$$\begin{aligned}
\nu_1 &= \big(720\xi_1(t_0) - 720\xi_1(t_f) + 360\xi_2(t_0)t_f + 360\xi_2(t_f)t_f \\
&\quad +60\xi_3(t_0)t_f^2 - 60\xi_3(t_f)t_f^2\big)/t_f^5 \\
\nu_2 &= \big(-360\xi_1(t_0) + 360\xi_1(t_f) - 168\xi_2(t_0)t_f - 192\xi_2(t_f)t_f \\
&\quad -24\xi_3(t_0)t_f^2 + 36\xi_3(t_f)t_f^2\big)/t_f^4 \\
\nu_3 &= \big(60\xi_1(t_0) - 60\xi_1(t_f) + 24\xi_2(t_0)t_f + 36\xi_2(t_f)t_f \\
&\quad +3\xi_3(t_0)t_f^2 - 9\xi_3(t_f)t_f^2\big)/t_f^3
\end{aligned} \tag{5.33}$$

Consequently, the undetermined multipliers are expressed in terms of initial and final conditions of the state variables and the final time, as shown in Eq. (5.33). Thus the constants of integration can be determined by substituting the solutions into Eq. (5.34), which is a rearranged form of Eq. (5.32).

$$\begin{aligned}
C_{\lambda_{\xi_1}} &= \nu_1 \\
C_{\lambda_{\xi_2}} &= C_{\lambda_{\xi_1}} t_f + \nu_2 \\
C_{\lambda_{\xi_3}} &= -\frac{1}{2} C_{\lambda_{\xi_1}} t_f^2 + C_{\lambda_{\xi_2}} t_f + \nu_3
\end{aligned} \tag{5.34}$$

The time histories of the state variables and the optimal control input in Eqs. (5.28) and (5.29) can be, therefore, determined. If initial and final conditions and a control time are given, the undetermined multipliers in Eq. (5.33) are determined, and they can be used to calculate the constants of integration in Eq. (5.34). Finally the constants of integration are substituted into Eqs. (5.28) and (5.29) to determine the time histories of the state variables and the optimal control input.

The significance of this analytical solution is that the optimal control problem of attitude control manoeuvres is solved completely and analytically including the boundary conditions at initial and final time. As mentioned above, the optimal spin rate control law can be determined immediately if initial and final conditions and a control time are given. Since there are only three constants of integration in the first three lines in Eq. (5.28), the time histories of the state variables can be determined uniquely.

5.4 Example Attitude Control Manoeuvres

Example attitude control manoeuvres are performed numerically in order to demonstrate the analytical solution.

Table 5.1 Example Attitude Control Manoeuvres.

	Initial attitude (ϕ, ψ) [deg]	Final attitude (ϕ, ψ) [deg]	Initial Spin Rate [rpm]	Final Spin Rate [rpm]	Time [day]
Case 1	(10, 30)	(30, 5)	1	1	2.08
Case 2	(15, 20)	(5, -30)	1	1	18.40
Case 3	(-10, -10)	(-25, -5)	1	1	21.45
Case 4	(-15, 5)	(-5, 5)	1	1	15.25
Case 5	(-10, -40)	(-5, 30)	1	1	57.30

The example attitude control manoeuvres examined are summarised in Table 5.1. Attitude at initial and final time is given arbitrarily. The initial and final spin rate is defined to be 1 rpm, for instance. The time taken for the attitude control is varied in a certain range, and the time that gives a solution with the minimum spin rate change is selected and written in Table 5.1. These boundary conditions and control time are substituted into the equations in the previous section to determine the control history.

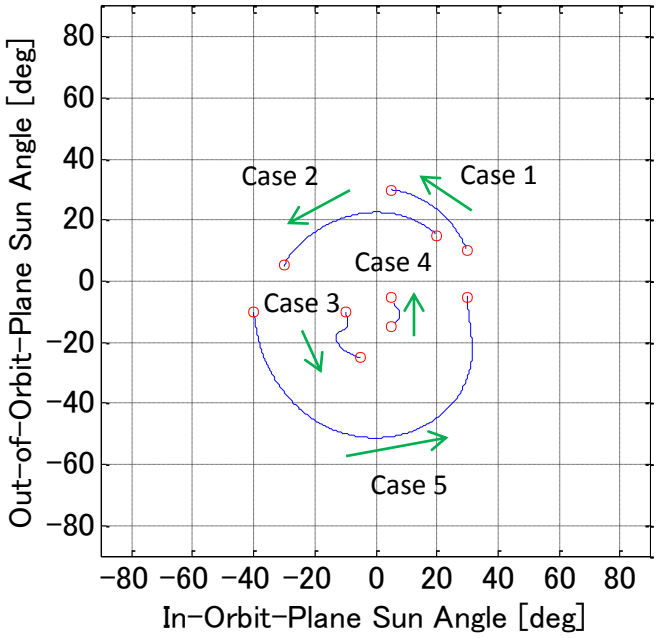

Fig. 5.1 Attitude History (Case 1, 2, 3, 4 and 5).

The attitude histories in the five control cases are plotted in Fig. 5.1. In general, it is not straightforward to determine the optimal spin rate control law that satisfies certain boundary

conditions; however, the unique time histories of the state variables and control input can be determined easily with the analytical solution if the boundary conditions are given.

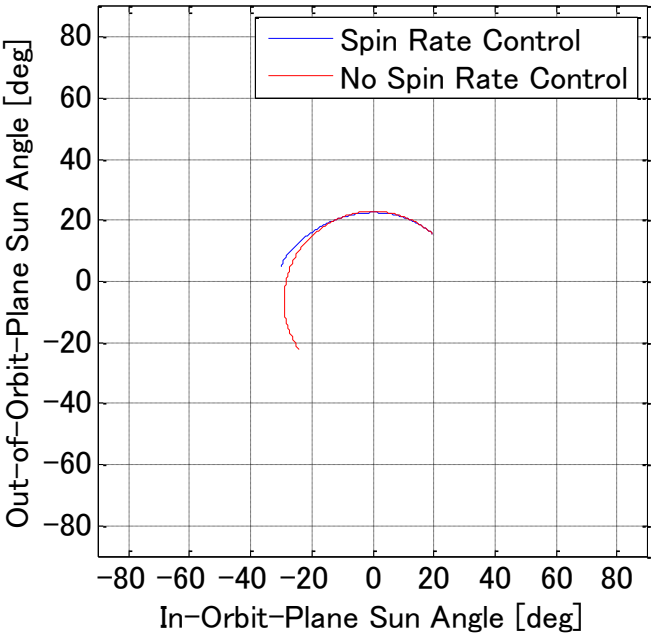

Fig. 5.2 Attitude History (Case 2).

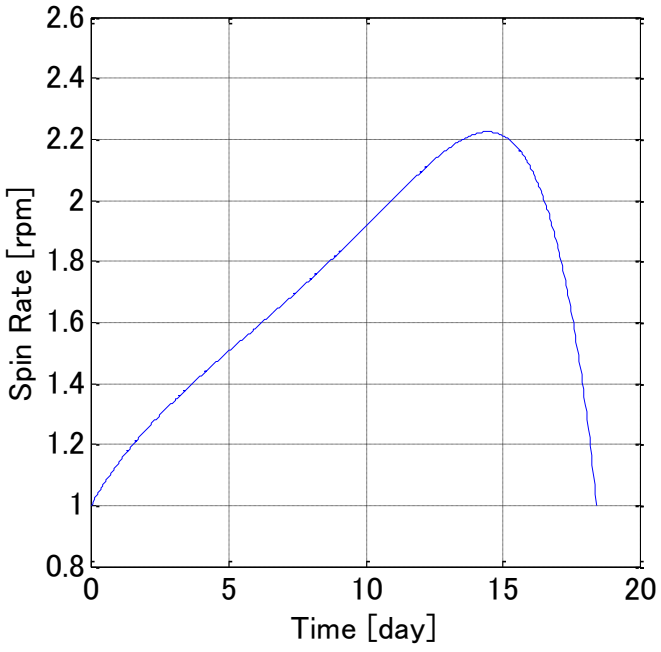

Fig. 5.3 Spin Rate History (Case 2).

Figures 5.2 and 5.3 show the attitude and spin rate histories in Case 2, for example, respectively. The red line in Fig. 5.2 shows the attitude history in a case where the spin rate is not controlled and remained at 1 rpm. It is simply a circular motion around an equilibrium direction, and the final attitude is not achieved. The blue line, on the other hand, shows the attitude history with appropriate spin rate control. The spin rate is controlled as shown in Fig. 5.3. As can be seen, the initial and final conditions of the attitude and spin rate are satisfied in Figs. 5.2 and 5.3.

In the cases summarised in Table 5.1, the attitude is always drifted even at the initial and final attitude due to the effect of solar radiation pressure. The attitude motion of a spinning solar sail is never fixed in the Sun-pointing coordinate system unless it is pointing exactly in the equilibrium direction. Now equilibrium direction-to-equilibrium direction attitude control is investigated.

Table 5.2 Example Equilibrium Direction-to-Equilibrium Direction Attitude Control Manoeuvres.

	Initial attitude (ϕ, ψ) [deg]	Final attitude (ϕ, ψ) [deg]	Initial Spin Rate [rpm]	Final Spin Rate [rpm]	Time [day]
Case 6	(-40, 0)	(-10, 0)	5.98	1.50	120.80
Case 7	(-5, 0)	(-30, 0)	0.75	4.49	77.40

Example equilibrium direction-to-equilibrium direction attitude control manoeuvres examined are summarised in Table 5.2. The initial and final spin rate is determined with the following equation from the initial and final attitude, respectively.

$$\Omega = \frac{pI_t}{\omega_s I_s}\phi_e \tag{5.36}$$

Eq. (5.36) shows the spin rate required to be pointing exactly in the equilibrium direction of $(-\phi_e, 0)$. Numerical simulation results are shown in the following figures.

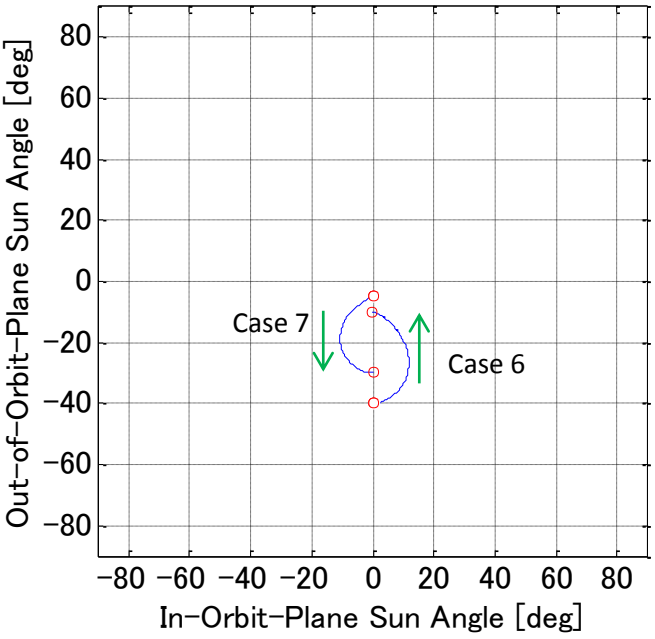

Fig. 5.4 Attitude History (Case 6 and 7).

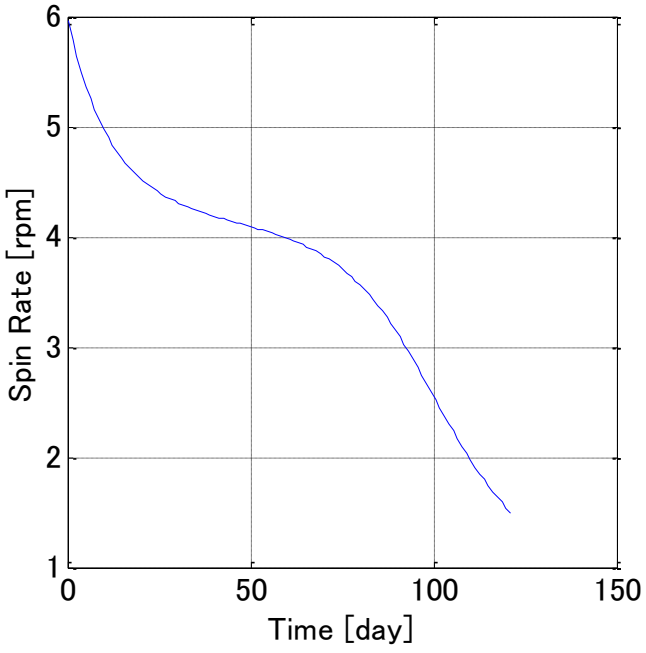

Fig. 5.5 Spin Rate History (Case 6).

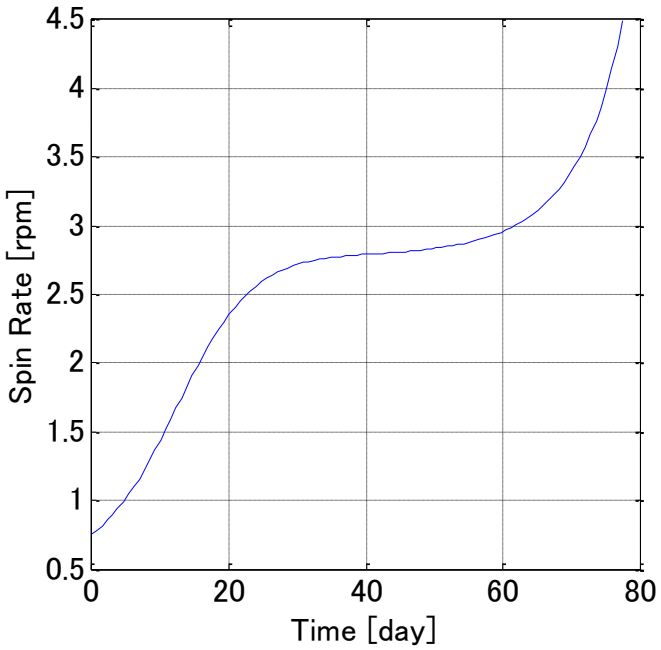

Fig. 5.6 Spin Rate History (Case 7).

Figure 5.4 shows the attitude histories of Case 6 and 7. The spin rate histories in the two cases are plotted in Figs. 5.5 and 5.6. As opposed to Case 1 to 5, the attitude drift motion is stopped at the initial and final attitude because the initial and final conditions of the spin rate are satisfied.

The equilibrium direction-to-equilibrium direction attitude control manoeuvres can only be performed by controlling the spin rate. It is possible to control the attitude of a spinning solar sail to an objective equilibrium direction also by generating a torque in a perpendicular direction to the spin-axis direction; however, the attitude motion does not stop at the objective equilibrium direction because the attitude continues to be drifted unless the angular momentum is balanced with the solar radiation pressure.

Moreover, an important point in this chapter is that an analytical solution of the equilibrium direction-to-equilibrium direction attitude control manoeuvres is determined and the manoeuvres can be realised with optimal yet simple spin rate control. The most conventional method to perform an equilibrium direction-to-equilibrium direction attitude control manoeuvre is to control the spin rate instantaneously from initial to final values that are set to track initial and final equilibrium directions respectively using chemical thrusters. If such spin rate control is performed, the spin-axis direction of a spacecraft starts rotating around the objective equilibrium direction, and the precession must be damped actively in order to point in the objective equilibrium direction eventually. The spin-axis direction continues to be drifted until the active damping is successfully performed. Hence the spin rate control law derived analytically and rigorously in this chapter is superior to the conventional control method. It is demonstrated that a control manoeuvre that is achieved with the sequence of spin rate control and precession damping in the conventional method can be performed with simple spin rate control in Figs. 5.5 and 5.6, for instance.

The significance of this chapter is that the effectiveness of the exact linearisation to solve a two-point boundary value problem is demonstrated. An optimal control problem of an originally bilinear system in Eq. (5.1) is solved analytically and rigorously by using the exact linearisation. In the next chapter, the exact linearisation is applied to orbit control of a spinning solar sail.

Chapter 6

Circular Orbit-to-Circular Orbit Transfer Optimisation

Since the work in this chapter is to be published as a peer-reviewed paper, it is deleted in this abridged version of thesis.

Chapter 7

Conclusions

In this thesis, the attitude and orbit control of a spinning solar sail by spin rate control is proposed. Since the attitude drift motion can be controlled by the spin rate, the attitude and orbital motions can be controlled indirectly by the spin rate through the attitude drift motion.

Firstly, it is shown that the acceleration and deceleration manoeuvres can be performed by the bang-bang control of the spin rate in Chapter 3. The simple spin rate control scheme can be used for orbit control of a spinning solar sail.

Secondly, in Chapter 4, the optimal spin rate control laws for orbital inclination maximisation, orbital eccentricity maximisation, aphelion maximisation and perihelion minimisation are determined. It is demonstrated that such control can be performed by the bang-bang control of the spin rate according to appropriate switching functions. With the results in Chapter 3, it is shown that the simple bang-bang control of the spin rate can perform several manoeuvres and generate optimal trajectories.

Thirdly, the nonlinear equations of the attitude drift motion are linearised using the exact linearisation in Chapter 5. The exact linearisation enables it to formulate an optimal control problem of attitude control manoeuvres that is analytically solvable, and the effectiveness of the exact lineatisation is demonstrated. In this Chapter, the equilibrium direction-to-equilibrium direction manoeuvres are also shown as examples.

Finally, a circular orbit-to-circular orbit transfer is optimised in Chapter 6. The attitude and orbital motions are dealt with simultaneously in the analytical derivation. This is enabled by the linearisation of the equations of motion using the exact linearisation. Globally optimal trajectories are also determined numerically, and it is shown that a spinning solar sail can be transferred to a circular orbit with a radius of 1.4 AU from 1 AU with the modest control of the spin rate. The numerical optimisation also shows that the final orbit radius can be maximised up to approximately 1.5 AU in the maximum-radius orbit transfer problem.

The work in this thesis can be divided into two major parts. In the first part, it is shown that the bang-bang control of the spin rate, which is optimal yet simple, can be applied to several orbit

control manoeuvres. This is useful in real-life operations because the control scheme is as straightforward as to switch maximum and minimum spin rate over to one after the other according to an appropriate switching function. In the second part, the exact linearisation is used to solve two-point boundary value problems. It is shown analytically and numerically that attitude and orbit control with initial and final boundary conditions to be satisfied can be realised only by controlling the spin rate.

The significance of this research is that a pure under-actuated system is investigated. The six degrees of freedom of the attitude and orbital motions are controlled by single control input, the spin rate. In other words, the attitude and orbit of a spinning solar sail is controlled by a minimum control degree of freedom. It provides ultimate redundancy and simplicity for a spinning solar sail because it enables the guidance and control of the spacecraft provided that only the spin rate is controllable. The control strategy proposed in this thesis, therefore, greatly contributes to the guidance and control of future spinning solar sails.

Appendix A

Parameters of IKAROS

The parameters of IKAROS are summarised in the table below.

Table A.1 Parameters of IKAROS

Mass	307 [kg]
Sail Area	184 [m^2]
Moment of Inertia around Spin Axis	404 [kgm^2]
Moment of Inertia around Perpendicular Axis to Spin Axis	780 [kgm^2]
Solar Radiation Pressure Parameter	3.68×10^{-7} [s^{-2}]
Specular Reflectivity	0.719
Diffuse Reflectivity	0.117
Absorptivity	0.162

The parameters of IKAROS are used for the calculation in this thesis. Only exceptions are the values of mass and sail area that are not used for orbital motion calculation. This is because the sail area-to-mass ratio of IKAROS is too low for orbit control using solar radiation pressure.

Appendix B

Orbital Elements Histories

Since the work in this appendix is to be published as a peer-reviewed paper, it is deleted in this abridged version of thesis.

References

[1] Maxwell, J. C., *Electricity and Magnetism*, Oxford University Press, 1873

[2] Lebedew, P., "The physical Causes of Deviation from Newton's Law of Gravitation," *Astrophysical Journal*, Vol. 10, 1902, pp. 155-161

[3] Tsiolkovsky, K. E., *Extension of Man into Outer Space*, 1921

[4] Mori, O., Sawada, H., Funase, R., Morimoto, M., Endo, T., Yamamoto, T., Tsuda, Y., Kawakatsu, Y., Kawaguchi, J., Miyazaki, Y., Shirasawa, Y., IKAROS Demonstration Team and Solar Sail Working Group, "First Solar Power Sail Demonstration by IKAROS," *Transaction of the Japan Society for Aeronautical and Space Science, Aerospace Technology Japan*, Vol. 8, No. ists27, 2010, pp. To_4_25-To_4_31

[5] Mori, O., Tsuda, Y., Sawada, H., Funase, R., Saiki, T., Yamamoto, T., Yonekura, K., Hoshino, H., Minamino, H., Endo, T., Kawaguchi, J., and IKAROS Demonstration Team, "IKAROS and Extended Solar Power Sail Missions for Outer Planetary Exploration," *Transaction of the Japan Society for Aeronautical and Space Science, Aerospace Technology Japan*, Vol. 10, No. ists28, 2012, pp. Po_4_13-Po_4_20

[6] Sawada, H., Mori, O., Okuizumi, N., Shirasawa, Y., Miyazaki, Y., Natori, M., Matunaga, S., Furuya, H., and Sakamoto, H., "Mission Report on The Solar Power Sail Deployment Demonstration of IKAROS," *Proceedings of the 52nd AIAA/ASME/ASCE/AHS/ASC Structures, Structural Dynamics and Materials Conference*, Denver, 2011

[7] Johnson, L., Whorton, M., Heaton, A., Pinson, R., Laue, G., and Adams, C., "NanoSail-D: A solar sail demonstration mission," *Acta Astronautica*, Vol. 68, No. 5-6, 2011, pp. 571-575

[8] Macdonald, M., *Advances in Solar Sailing*, Springer, 2014

[9] Cantrell, J., and Friedman, L., "Lightsail 1 – Flying for Less," *Proceedings of the Second International Symposium on Solar Sailing*, New York, 2010

[10] Lappas, V., Adeli, N., Visagie, L., Fernandez, J. M., Theodorou, T., Steyn, W., and Perren, M., "CubeSail: A low cost CubeSat based solar sail demonstration mission," *Advances in Space Research*, Vol. 48, No. 11, 2011, pp. 1890-1901

[11] Funase, R., Mori, O., Shirasawa, Y., and Yano, H., "Trajectory and System Design for Jovian Trojan Asteroid Exploration Using Solar Power Sail," *29th International Symposium on Space Technology and Science*, Nagoya, 2013

[12] Kawaguchi, J., and Shirakawa, K., "A Fuel-Free Sun-Tracking Attitude Control Strategy and the Flight Results in Hayabusa (MUSES-C)," *Proceedings of the 17th AAS/AIAA Space Flight Mechanics Meeting*, Sedona, 2007

[13] Tsuda, Y., Saiki, T., Funase, R and Mimasu, Y., "Generalized Attitude Model for Spinning Solar Sail Spacecraft," *Journal of Guidance, Control, and Dynamics*, Vol. 36, No. 4, 2013, pp. 967-974

[14] Funase, R., Mimasu, Y., Shirasawa, Y., Tsuda, Y., Saiki, T., and Kawaguchi, J., "Modelling and On-orbit Performance Evaluation of Propellant-free Attitude Control System for Spinning Solar Sail via Optical Parameter Switching," *Proceedings of the 2011 AAS/AIAA Astrodynamics Specialist Conference*, Girdwood, 2011

[15] Saiki, T., Tsuda, Y., Funase, R., Mimasu, Y., Shirasawa, Y., and IKAROS Demonstration Team, "Attitude operation Results of Solar Sail Demonstrator IKAROS," *Transaction of the Japan Society for Aeronautical and Space Science, Aerospace Technology Japan*, Vol. 10, No. ists28, 2012, pp. To_4_1-To_4_6

[16] Mimasu, Y., Yamaguchi, T., Nakamiya, M., Ikeda, H., Funase, R., Saiki, T., Tsuda, Y., and Kawaguchi, J., "Orbit Steering Method of Solar Sail via Spin Rate Control," *Proceedings of the 28th International Symposium on Space Technology and Science*, Okinawa, 2011

[17] Mimasu. Y., Yamaguchi, T., Nakamiya, M., Ikeda, H., Funase, R., Saiki, T., Tsuda, Y., and Kawaguchi, J., "Orbit Control Method for Solar Sail Demonstrator IKAROS via Spin Rate Control," *Proceedings of the 2011 AAS/AIAA Astrodynamics Specialist Conference*, Girdwood, 2011

[18] Mimasu, Y., Yamaguchi, T., Matsumoto, M., Nakamiya, M., Funase, R., and Kawaguchi, J., "Spinning Solar Sail Orbit Steering Via Spin Rate Control," *Advances in Space Research*, Vol. 48, Issue 11, 2011, pp. 1810-1821

[19] Enright, P.J., and Conway, B.A., "Optimal Finite-Thrust Spacecraft Trajectory Using Collocation and Nonlinear Programming," *Journal of Guidance, Control and Dynamics*, Vol. 14, No. 5, 1991, pp. 981-985

[20] Hargraves, C.R., and Paris, S.W., "Direct Trajectory Optimization Using Non-linear Programming and Collocation," *Journal of Guidance, Control and Dynamics*, Vol. 10, No. 4, 1987, pp. 338-342

[21] Kawaguchi, J., "HAYABUSA-A New Solar System Cruiser," *Proceedings of the 25th International Symposium on Space Technology and Science*, Kanazawa, 2006

[22] Tsuchiyama, A., Uesugi, M., Matsushima, T., Michikami, T., Kadono, T., Nakamura, T., et al., "Three-Dimensional Structure of Hayabusa Samples: Origin and Evolution of Itokawa Regolith," *Science*, Vol. 333, No. 6046, 2011, pp. 1125-1128

[23] Yurimoto, H., Abe, K., Abe, M., Ebihara, M., Fujimura, A., Hashiguchi, M., et al., "Oxygen Isotopic Compositions of Asteroidal Materials returned from Itokawa by the Hayabusa Mission," *Science*, Vol. 333, No. 6046, 2011, pp. 1116-1119

[24] Kawaguchi, J., Kominato, T., and Shirakawa, K., "Attitude Control Flight Experience: Coping with Solar Radiation and Ion Engines Leak Thrust in Hayabusa (MUSES-C)," *Proceedings of the 20th International Symposium on Space Flight Dynamics*, Annapolis, 2007

[25] Ono, G., Mimasu, Y., and Kawaguchi, J., "Attitude Optimisation of a Spinning Solar Sail via Spin-Rate Control to Accelerate in Tangential Direction," *Proceedings of the 23rd AAS/AIAA Space Flight Mechanics Meeting*, Kauai, 2013

[26] Bryson, A.E. Jr., and Ho, Y.C., *Applied Optimal Control*, Hemisphere Publishing Corporation, 1975

[27] Ono, G., Mimasu, Y., and Kawaguchi, J., "Attitude Control of a Spinning Solar Sail via Spin Rate Control using Exact Linearization," *Transactions of the Japan Society for Aeronautical and Space Sciences Aerospace Technology Japan*, Vol. 12, No. ists29, 2014, pp. Pd_27-Pd_32

[28] Isidori, A., *Nonlinear Control Systems*, Springer, 1995

[29] Jakubczyk, B., and Rspondek, W., "On Linearization of Control Systems," *Bull. Acad. Polonaise Sci. Ser. Sci. Math.*, Vol. 28, 1980, pp. 517-522

[30] Su, R., "On the Linear Equivalents of Nonlinear Systems," *Systems and Control Letters*, Vol. 2, No.1, 1982, pp. 48-52

[31] Hunt. L.R., Su, R., and Meyer, G., "Design for Multi-Input Nonlinear Systems," *Differential Geometric Control Theory*,1982, pp. 268-298